Trapping of water waves by moored bodies

by J. N. Newman
<jnn@mit.edu>

(Submitted to J Eng Math – September 19, 2007)

Abstract Certain types of floating bodies are known to support trapped modes, with oscillatory fluid motion near the body and no energy radiation in the far field. Previous work has considered either fixed bodies, where the boundary conditions are homogeneous, or bodies which are freely floating and moving without any exciting force. For a fixed body the existence of a trapped mode implies that there is no unique solution of the boundary-value problem for the velocity potential with a prescribed body motion. For a free body which supports a trapped mode, the solution of the coupled problem for the motions of the fluid and body does not have a unique solution. A more general case is considered here, of a body with a linear restoring force such as an elastic mooring. The limiting cases of a fixed and free body correspond to infinite or zero values of the corresponding spring constant. A variety of body shapes are found including cylinders in two dimensions and axisymmetric bodies in three dimensions, which illustrate this more general case of trapping and provide a connection between the fixed and free cases.

Keywords Floating bodies – Water waves – Trapped modes – Uniqueness

1 Introduction

In the linear theory of wave interactions with floating bodies, the velocity potential is governed by Laplace's equation in the fluid domain, a mixed boundary condition on the free surface, and vanishing of the potential at large depths (or, if the depth is finite, vanishing of the normal velocity on the bottom). A radiation condition is applied in the far field. On the submerged surface of the body an inhomogeneous Neumann condition is applicable, stipulating that the normal velocities of the body and fluid are equal (or, in the diffraction problem, that the normal derivative of the scattering potential cancels the normal component of the incident-wave velocity).

This boundary-value problem has been studied extensively over the past century [1,2,3,4]. Numerous applications exist, particularly in offshore engineering [5]. One topic of special interest from the theoretical standpoint is the issue of uniqueness. John [6] provided a proof of uniqueness with some restrictions on the body shape, and various extensions have been made, but there is no general proof for this class of boundary-value problems. Recent reviews of this subject can be found in [7] and [8].

The impossibility of a general proof of uniqueness was established by McIver [9]. She showed by an indirect approach that special body profiles exist in two dimensions, with the property

that a trapping mode is supported at a discrete frequency. This is a mode of fluid motion with finite energy, which persists in the presence of a *fixed* body and does not radiate energy to infinity. Thus it is a solution of the linear boundary-value problem with homogeneous boundary conditions. Since an arbitrary multiple of this solution can be added to particular solutions of physically-relevant problems, its existence implies that the solution is not unique. McIver's approach has been used subsequently to show that a variety of fixed trapping structures exist in both two and three dimensions [10,11,12].

Recently McIver and McIver [13,14] have shown that similar structures exist which support trapped modes when they are freely floating and moving in an oscillatory manner, without the restraint of external forces. This is a different situation from the physical standpoint, describing the dynamics of a floating body which is excited by an oscillatory force such as the action of the incident wave system. From the practical standpoint, the existence of a trapping mode in this context implies that there is no unique solution of the equations of motion. The terms 'sloshing trapping structure' and 'motion trapping structure' are used in [13] and [14] to distinguish between these two complementary problems, where the body is fixed or free, respectively.

The two-dimensional constructions in [9] and [13] are based on tracing the streamlines generated by two symmetrical singularities on the free surface, which are separated by one-half wavelength (or, more generally, an integer plus one-half wavelengths). Thus there are no radiated waves in the far field. For the fixed structure a pair of wave sources is used. For the free structure, wave sources and wave-free singularities are combined, such that the total dipole moment vanishes in the far field, and it follows from Green's theorem that non-zero body motions can exist without an exciting force. The axisymmetric three-dimensional extensions [10,14] are analogous, with the singularities distributed on a circular ring in the plane of the free surface; if the product of the wavenumber and ring radius is a zero of the Bessel function J_0, there is complete cancelation of the radiated waves as in the two-dimensional case.

The fixed and free trapping structures which result from these constructions have two features in common: (a) there is an interior region of fluid or 'moonpool' which is connected to the exterior domain beneath the body but enclosed by the body on the free surface, and (b) the vertical component of the vector normal to the body surface changes sign below the free surface, so that the body slopes up and inward where it intersects the free surface on the exterior side. Other techniques have been used to establish that fixed and free trapping structures exist without the latter feature [15, 16].

In the present work a connection is made between the fixed and free trapping problems, by considering the more general case where a floating body is restrained by a linear restoring force, as in the case of an idealized elastic mooring. Free trapping structures are recovered in the limit where the restoring coefficient (or 'spring constant') $k = 0$. Conversely, if $k \to \pm\infty$, fixed trapping structures are recovered. (The case $k \to +\infty$ is more obvious from the physical standpoint, corresponding to a fixed restraint. The limit $k \to -\infty$ corresponds to an infinitely large inertial restraint; since this also prevents any motion it is admissible as a limit where the body is fixed.)

For the more general case ($0 < |k| < \infty$) we use a linear combination of the singularities required in the two complementary limits. One minor change from the analysis in [13] and [14] is the use of quadrupoles to represent the component associated with free trapping structures, instead of the combination of wave sources and wave-free singularities. That particular combination of singularities, with zero dipole moment in the far field, is equivalent to a vertical

quadrupole, as shown in Appendix A. Thus we consider here the streamlines and possible body contours generated by sources and quadrupoles.

Separate analyses are described below for the two-dimensional and axisymmetric three-dimensional problems. The fluid is assumed to be ideal, and unbounded except for the free surface and the submerged surface of a floating body which has finite dimensions. The motions of the body and fluid are harmonic in time, with small amplitudes. Only vertical (heave) motions of the body are considered. The solution for the velocity potential is constructed from appropriate combinations of sources and quadrupoles, and the corresponding streamlines are traced by numerical procedures. A variety of trapping structures are found, depending on the parameter k. In some cases, where k is large and positive, bodies are discovered which do not have an interior free surface. Conversely, when k is large and negative, bodies are found where the vertical component of the vector normal to the body surface does not change sign.

2 Analysis in two dimensions

The motion is harmonic with frequency ω in the plane x, z, where $z = 0$ is the free surface and z is positive upwards. The coordinates are nondimensionalized with respect to the wavenumber $K = \omega^2/g$, where g is the gravitational acceleration. Thus the wavelength is 2π and the free-surface condition is $\phi - \phi_z = 0$ on $z = 0$. We define the complex variable $Z = z + \mathrm{i}x$ and the complex potential $F = \phi + \mathrm{i}\psi$, where ϕ is the velocity potential and ψ the stream function.

For a pair of point sources of oscillatory strength, situated at the points $x = \pm\pi/2$ on the free surface, the complex potential can be expressed in the form

$$F_s = \mathrm{e}^{(Z+\mathrm{i}\pi/2)}\mathrm{E}_1(Z + \mathrm{i}\pi/2) + \mathrm{e}^{(Z-\mathrm{i}\pi/2)}\mathrm{E}_1(Z - \mathrm{i}\pi/2) - 2\pi\mathrm{H}(\pi/2 - |x|)\mathrm{e}^Z. \tag{1}$$

Here E_1 is the exponential integral, defined as in [17], and $\mathrm{H}(\pi/2-|x|)$ is equal to 1 if $|x| < \pi/2$, otherwise zero. The oscillatory time-dependence has been factored out, taking advantage of the fact that the usual out-of-phase components of the oscillatory source potential are canceled by the half-wavelength spacing. For a pair of quadrupoles at the same points, the complex potential is

$$F_q = \frac{d^2 F_s}{dZ^2}. \tag{2}$$

Using the asymptotic expansion for the exponential integral ([17] equation 5.1.51), it follows that $F_s \simeq 2Z^{-1}$ and $F_q \simeq 4Z^{-3}$ as $|Z| \to \infty$. Thus F_s is 'dipole-like' in the far field, and F_q is a higher-order singularity with zero dipole moment.

Following the analysis of a freely-floating structure in [13], the solution of the equation of motion for heave will admit nontrivial homogeneous solutions if (a) there is no damping, and (b) the sum of the inertial and restoring forces is zero. Zero damping is ensured for any motions associated with the singularities (1) and (2), since there is no radiated wave energy. The second condition corresponds to the equation (cf. [13], equation 4)

$$\rho g W(1 + k) - \omega^2(M + a) = 0. \tag{3}$$

Here $\rho g W$ is the hydrostatic restoring force with ρ the fluid density and W the width of the waterplane, and k is a nondimensional external restoring coefficient. M is the body mass and a the added mass. From Green's theorem it can be shown ([13], equation 18) that

$$\rho g W - \omega^2(M + a) = -\pi\mu\rho\omega^2, \tag{4}$$

where μ is the far-field dipole moment, defined such that the asymptotic approximation of the potential ϕ_0 for unit heave velocity is

$$\phi_0 \simeq -\mu K \mathrm{Re}(Z^{-1}) \quad \text{as} \quad |Z| \to \infty. \tag{5}$$

Thus, for a body with an external restoring force, a necessary condition for a trapping mode to exist is

$$k = \pi \mu K / W. \tag{6}$$

Following the constructions in [9] and [13] we consider the streamlines ψ =constant, associated with the complex potential

$$F = SF_s + QF_q - V(Z+1). \tag{7}$$

Here S is the source strength, Q the quadrupole strength, and V represents a vertical streaming velocity at infinity which is introduced to cancel the equal and opposite velocity of the body. F, S, Q, V are nondimensionalized by ω and g. S, Q, and V are real. Without loss of generality it can be assumed that $V \geq 0$.

As $|Z| \to \infty$,

$$F \simeq 2S/Z - V(Z+1)$$

and the (dimensional) dipole moment for unit heave velocity is

$$\mu = -2S/K^2 V. \tag{8}$$

From (6) it follows that

$$k = -(2\pi S/KWV). \tag{9}$$

Thus, for a positive restoring coefficient, the source strength S must be negative (corresponding to a source with positive flux). Conversely, if $S > 0$ (a sink), the mooring restraint is inertial.

Streamlines which surround the singular points $x = \pm\pi/2$ below the free surface will correspond to the profiles of trapping structures moving with vertical velocity $(g/\omega)V$. By tracing the streamlines numerically, it can be shown that such profiles do in fact exist, for most but not all combinations of the parameters S, Q, V. Since (7) can be multiplied by an arbitrary real constant without affecting the streamlines, only the relative values of S, Q, V are relevant and the parameter space is two-dimensional.

3 Streamlines and body profiles

The computations for the streamlines are based on searching with a Newton-Raphson procedure for the loci of points with constant values of the stream function, starting at the stagnation point and continuing until the streamlines intersect the free surface on both sides of the body. The complex potential (1) is evaluated using a double-precision subroutine for the complex exponential integral based on the ascending series and continued fraction expansions in [17]. Derivatives up to fourth order are evaluated recursively, as in equation 30 of Appendix B. Step lengths between 10^{-1} and 10^{-2} are used. The maximum errors in the coordinates of the body profiles are on the order of 10^{-4}.

If $V = 0$ and $Q = 0$ the streamlines of (7) yield the family of profiles shown in Figure 1(a). Conversely, if $S = 0$ the dipole moment $\mu = 0$, and it follows from (6) that the body is free. For this case a one-parameter family of closed streamlines exists, depending on the ratio Q/V, with profiles shown in Figure 1(b). Except for the normalization of the coordinates these are graphically identical to the profiles derived in [9] and [13] respectively.

In order to reduce the number of independent parameters we first consider the case $Q = V$ and, without loss of generality except for the scale, set $Q + |S| = 1$. (This permits us to cover all possible finite values of Q/S with $-1 < S < 1$.) Examples of the streamlines are shown in Figure 2, with the corresponding values of the restoring coefficient k. In the left column $S < 0$ and $k > 0$, and conversely in the right column. In all cases shown there is at least one streamline which surrounds the singular point $x = \pi/2$ in the domain below the free surface, and thus defines the profile of a trapping structure. For small values of S and k this profile is similar to the case $S = 0$, shown by the dashed curve in Figure 1(b). In this regime only one profile exists, with a stagnation point where it intersects the dividing streamline. As $|S|$ increases the stagnation point and dividing streamline shift toward the right ($S > 0$) or left ($S < 0$), with more significant changes. For $S = 0.7$ (approximately) the right side of the body profile is vertical at the free surface and for $S > 0.7$ the vertical component of the interior normal vector is positive at all points. In this regime trapping structures exist which satisfy one of John's uniqueness requirements for fixed structures, that no vertical lines starting in the free surface intersect the body. On the other hand, for $S \leq -.7$ the stagnation point is on the vertical axis and the body profile which intersects this point is continuous with its reflection in $x < 0$; thus a single closed body is generated without an interior free surface. In both cases, for larger values of $|S|$, a family of additional streamlines surround the singular point within the interior of the profile which intersects the stagnation point; in the limit $S \to \pm 1$ ($Q = V \to 0$) this family corresponds to the profiles of the fixed trapping structures shown in Figure 1(a).

Additional computations have been made which confirm the existence of similar profiles throughout the parameter range $-0.9 \leq S \leq 0.9$ and $0.1 \leq Q/V \leq 10$. In general, the profiles are smaller and closer to the singular point when Q/V is large, and *vice versa*.

Figure 3 shows profiles of moving bodies generated by sources only, without quadrupoles. These profiles are similar to those shown in the lower row of Figure 2. For small negative values of S/V there is no profile, but for $S < -0.8V$ a profile exists that is similar to the lower left plot in Figure 2, with no interior free surface. Note that in the latter case the source flux is positive, and the streaming flow is downward. It is remarkable that a closed body is formed in this case, downstream of the pair of sources, contrary to the orientation of a semi-infinite half-body in an infinite fluid (cf. [18], Figure 4.1).

Figure 4 shows profiles of fixed bodies where both sources and quadrupoles are used. For $Q/S > 0$ there is apparently no upper bound on Q/S, but the domain $Q/S > 10$ has not been explored. For small negative values of Q/S similar families also exist, but this range is limited to, approximately, $-0.6 < Q/S < 0$. Within these ranges, sources and quadrupoles can be combined to generate fixed trapping structures which generalize from the results in [1]. The principal effect of the quadrupoles is to induce a stagnation point on the innermost body profile.

4 Axisymmetric trapping structures

A similar analysis can be made for the axisymmetric three-dimensional case, extending the results in [14]. Nondimensional polar coordinates (r, z) are used. Sources of strength S and quadrupoles of strength Q are distributed uniformly around a circular ring of radius $r = j_{0,1}$ in the plane of the free surface, where $j_{0,1} = 2.4048..$ is the first zero of the Bessel function J_0. Including the vertical streaming flow as in (7), the velocity potential is

$$\phi = S\phi_s + Q\phi_q - V(z+1) = \left(S + Q\frac{\partial^2}{\partial z^2}\right)\phi_s - V(z+1), \tag{10}$$

where

$$\phi_s = \int_0^{2\pi} G(x, y, z; r\cos\alpha, r\sin\alpha, 0) r d\alpha. \tag{11}$$

The Green function G is defined in Appendix B.

In this case the right side of (4) includes the factor 2 (cf. [14], equation 15), and (6) is replaced by

$$k = 2\pi\mu K/W. \tag{12}$$

Here W is the body's waterplane area, and the dipole moment μ is defined such that the potential for unit heave velocity is

$$\phi_0 \simeq \mu\cos\theta/R^2 \quad \text{as} \quad R \to \infty, \tag{13}$$

with R the dimensional spherical radius from the origin and θ the angle from the negative z-axis. Using equation 32 in Appendix B, the leading term in the asymptotic expansion of (11) is

$$\phi_s \simeq -4\pi j_{0,1}\cos\theta/K^2R^2. \tag{14}$$

Thus

$$\mu = -4\pi j_{0,1} S/(K^3 V) \tag{15}$$

and

$$k = -8\pi^2 j_{0,1} S/(K^2 W V). \tag{16}$$

For the present computations, the potential and first derivatives of the three-dimensional ring source are evaluated in the same manner as described in [11], using a double-precision subroutine for the point source and integrating around the circular ring with adaptive Gauss-Chebyshev integration. Higher-order derivatives are evaluated recursively, as in equation 30 of Appendix B.

The coordinates of stream surfaces are determined based on the direction of the velocity vector, with a second-order correction based on the velocity at the midpoint of each step. Step lengths between 10^{-3} and 2.5×10^{-4} are used. The maximum errors in the coordinates of the body profiles are on the order of 10^{-4}.

Figure 5 shows examples of the body profiles where $Q = V = 1 - |S|$. These are similar to the two-dimensional profiles illustrated in Figure 2.

Computations of the added mass, damping, and exciting-force coefficients for these structures have been performed in order to verify that the homogeneous equation of motion (3) is

satisfied at the trapping point $K = 1$, with no damping at this point, and to characterize the hydrodynamic forces at other wavenumbers. For this purpose the radiation/diffraction code WAMIT is used [19]. The geometry of the bodies is represented analytically, with each profile represented by an economized polynomial of degree ten. For bodies with an internal free surface the polynomial is in powers of the polar angle about the singular point, ranging from 0 to π to cover the submerged portion of the profile. For bodies without an internal free surface the polar angle is about the origin, ranging from zero on the free surface to $\pi/2$ on the vertical axis. The economized polynomials are derived from Chebyshev expansions which fit the computed streamline coordinates with maximum errors on the order of 10^{-4}. Cubic B-splines are used to represent the velocity potential. The results shown are estimated to be accurate to three decimals.

Figure 6 shows the force coefficients for the case $S = 0$, where the body is free, as in [14]. In addition to the added-mass and damping coefficients, Figure 6(a) also shows the real part of the left-hand side of the equation of motion (3), confirming that it vanishes at the point $K = 1$. The damping coefficient vanishes at this point, as expected, and also at $K \simeq 1.1$. The latter feature is apparently due to the outer profile of the body, and analogous to other bodies which have their maximum radius below the free surface. To confirm this point computations have been made for the same profile, but with the interior free surface replaced by a circular disk which is part of the body; for this structure the damping coefficient vanishes at $K \simeq 1.15$. The real and imaginary parts of the exciting force are plotted in Figure 6(b), to give more precise indications of the points where the damping is zero; it follows from the Haskind relations [18] that the exciting force and damping vanish at the same point, and since the real and imaginary parts of the exciting force change sign this point is indicated more clearly in Figure 6(b).

Figure 7 shows the same coefficients as in Figure 6(a), for the cases $S = \pm 0.7$. The corresponding profiles are shown in Figure 5. For $S = +0.7$ where an interior free surface is present, sharp fluctuations occur in the vicinity of $K = 1$. In this case the restoring force required to produce trapping at $K = 1$ is negative. For $S = -0.7$, where a positive restoring force is required to produce trapping, there is no internal free surface and the force coefficients do not fluctuate rapidly.

5 Discussion and conclusions

The existence of a trapping mode has been established numerically for floating bodies which are restrained by linear elastic restoring forces. The restoring force is represented by a coefficient k, equivalent to a spring constant. Examples of structures which support these modes are derived by an indirect procedure, where the fluid motion is generated by sources and vertical quadrupoles located at singular points on the free surface. The geometry of the structures is represented by profiles which correspond to specific streamlines in the fluid. These streamlines separate the fluid domain outside the body from the singular points inside the body. The analysis is carried out both in two dimensions and for axisymmetric structures in three dimensions, with similar results.

In the limit $k \to 0$ the body is free, and the results correspond to the free trapping structures discovered by McIver and McIver [13,14]. Conversely, for $k \to \pm\infty$ the body is fixed, and the streamlines correspond to the fixed trapping structures discovered by the same authors [9,10]. The parameter k provides a connection between these two complementary limits, and shows

that trapping structures also exist in the intermediate regimes. From the practical standpoint, $k > 0$ is relevant to a moored vessel where the mooring can be represented by a linear spring. The regime $k < 0$ would be applicable to a vessel which is restrained by a mechanical device with effective inertia.

As noted in the Introduction, the existence of a trapping mode implies that there is no unique solution of the boundary-value problem for the potential, or of the equations of motion for the moving body.

The profiles of trapping structures for small values of k are similar to the structures found by McIver and McIver [13,14] for $k = 0$. One might expect a similar correspondence for larger values of $|k|$ with the fixed trapping structures. However significant differences are found in the latter case. For large positive values of k the interior fluid region is absent, and for large negative values the vertical component of the normal vector on the submerged body surface does not change sign. The existence of a trapping structure without an interior 'moonpool' is particularly interesting, since this has been a feature of all fixed and free floating bodies which support a trapped mode [14].

The restoring force considered here acts in the vertical (heave) direction, and this is the only degree of freedom considered for the body motion. The situation is more complicated for the general case of six degrees of freedom of a rigid body, but for symmetric bodies heave is uncoupled from the other modes. Thus a trapping mode associated with heave implies that there is no unique solution of the equation of motion for heave, regardless of whether the other modes are fixed, free, or restrained. Similar trapping modes have been found for horizontal motions of free bodies [13].

There is a wide variety of bodies which do not radiate waves in the far field, when oscillated in an appropriate manner at one particular frequency. Examples include 'bulbous' bodies, where the maximum width or radius is below the free surface, such that there is complete cancelation of the radiated waves due to heave motions. Bodies of this type were described by Bessho [20] and Motora and Koyama [21]. See also the discussions of [21].

An extensive study of wave-free structures was performed by Kyozuka and Yoshida [22], where the streamlines are generated by wave-free singularities on the vertical axis below the free surface. Their work includes comparisons with experiments in both two and three dimensions. They also considered the heave response when the body is moored, with the restoring coefficient tuned for resonance at the frequency of zero damping. In that condition their problem is equivalent to that studied here, although they did not consider trapping specifically and the class of bodies generated by their singularities does not include the possibility of a moonpool.

Other examples of wave-free structures include symmetric bodies with suitable combinations of horizontal translation and rotation (or rotation about a particular axis), such that the radiated waves in the two modes of motion cancel. It is evident that any wave-free structure can support trapped modes if it is restrained by a suitable restoring force. The only requirement, in addition to zero energy radiation, is for the value of the restoring coefficient k to cancel the remaining terms in the equation of motion (3). Thus it is not surprising to find that a moored body without an internal free surface can support a trapped mode. This argument also suggests that axisymmetry is not necessary in three dimensions.

References

1. Wehausen JV, Laitone EV (1960) Surface Waves. In: Flügge S (ed.), Encyclopedia of Physics, 9:446-778. (Available for download from www.coe.berkeley.edu/SurfaceWaves)
2. Mei CC (1989) The applied dynamics of ocean surface waves, 2nd edition. World Scientific Pub Co, Singapore
3. Linton CM, McIver P (2001) Handbook of Mathematical Techniques for Wave/Structure Interactions. Chapman & Hall/CRC, London
4. Evans DV (2004) Mathematical techniques for linear wave-structure interactions. In: Landrini M *et al* (eds.), Proceedings of the 19th International Workshop on Water Waves and Floating Bodies, Cortona, Italy. (Available for download from www.iwwwfb.org)
5. Faltinsen OM (1991) Sea loads on ships and offshore structures. Cambridge University Press, Cambridge, UK
6. John F (1950) On the motion of floating bodies, II. Communications on Pure and Applied Mathematics 3:45-101
7. Kuznetsov N, Maz'ya V, Vainberg B (2002) Linear Water Waves. Cambridge University Press, Cambridge, UK
8. Linton CM, McIver P (2007) Embedded trapped modes in water waves and acoustics. Wave Motion (in press)
9. McIver M (1996) An example of non-uniqueness in the two-dimensional linear water wave problem. J Fluid Mechanics 315:257-266
10. McIver P, McIver M (1997) Trapped modes in an axisymmetric water-wave problem. Quarterly Journal of Mechanics and Applied Mathematics 50:165-178
11. Newman JN (1999) Radiation and diffraction analysis of the McIver toroid. J Eng Math 35:135-147
12. McIver P, Newman JN (2003) Trapping structures in the three-dimensional water-wave problem. J Fluid Mechanics 484:283-301
13. McIver P, McIver M (2006) Trapped modes in the water-wave problem for a freely floating structure. J Fluid Mechanics 558:53-67
14. McIver P, McIver M (2007) Motion trapping structures in the three-dimensional water-wave problem. J Eng Math 58:67-75
15. Shipway BJ, Evans DC (2003) Wave trapping by axisymmetric concentric cylinders. J Offshore Mechanics and Arctic Engineering 125:59-64
16. Evans DV, Porter R (2007) Examples of motion trapped modes in two and three dimensions. In: Malenica S, Senjanovic I (eds.), Proceedings of the 22nd International Workshop on Water Waves and Floating Bodies, Plitvice, Croatia. (Available for download from www.iwwwfb.org)
17. Abramowitz M, Stegun I (1964) Handbook of Mathematical Functions. National Bureau of Standards, Washington
18. Newman JN (1977) Marine Hydrodynamics. MIT Press, Cambridge, USA

19. Lee C-H, Newman JN (2005) Computation of wave effects using the panel method. In: Chakrabarti S (ed.) Numerical Models in Fluid Structure Interaction.WIT Press, Southampton, pp 211-251

20. Bessho M (1967) On the theory of wave-free ship forms. Memoirs of the Defense Academy, Japan 7,1:263-277

21. Motora S, Koyama T (1966) Wave excitationless ship forms. In Cooper R, Doroff S (eds.) Proceedings of the Sixth Symposium on Naval Hydrodynamics. US Government Printing Office, Washington pp 383-413

22. Kyozuka Y, Yoshida K (1981) On wave-free floating-body forms in heaving oscillation. Applied Ocean Research 3,4:183-194

23. Newman JN (1985) Algorithms for the free-surface Green function. J Eng Math 19:57-67

Appendix A – Two-dimensional singularities in the free surface

Dimensional coordinates are used here for the sake of perspicuity. The potential of a wave source with oscillatory strength $\cos\omega t$, located at the point $x=\xi, z=\zeta$, can be expressed in the form

$$\phi_s = [\log(r/r_1) - 2\mathrm{Re}(F)]\cos\omega t - 2\pi\mathrm{Re}\left(\mathrm{e}^Z\right)\sin\omega t, \tag{17}$$

where

$$\begin{pmatrix} r \\ r_1 \end{pmatrix} = \sqrt{(x-\xi)^2 + (z \mp \zeta)^2},$$

$$F = \mathrm{e}^Z\left[\mathrm{E}_1(Z) + \pi\mathrm{i}\right],$$

and $Z = K\left(z+\zeta+\mathrm{i}(x-\xi)\right)$. The corresponding expressions for the vertical dipole and quadrupole are

$$\phi_d = \frac{\partial\phi_s}{\partial\zeta} = \left[-\frac{z-\zeta}{r^2} - \frac{z+\zeta}{r_1^2} - 2K\mathrm{Re}(F')\right]\cos\omega t - 2\pi K\mathrm{Re}\left(\mathrm{e}^Z\right)\sin\omega t \tag{18}$$

and

$$\begin{aligned}\phi_q &= \frac{\partial^2\phi_s}{\partial\zeta^2} = \frac{\partial^2\phi_s}{\partial z^2} \\ &= \left[\frac{1}{r^2} - \frac{1}{r_1^2} - 2\frac{(z-\zeta)^2}{r^4} + 2\frac{(z+\zeta)^2}{r_1^4} - 2K^2\mathrm{Re}(F'')\right]\cos\omega t \\ &\quad -2\pi K^2\mathrm{Re}\left(\mathrm{e}^Z\right)\sin\omega t,\end{aligned} \tag{19}$$

where F' and F'' denote the derivatives with respect to Z. When $\zeta = 0$ these equations simplify as follows:

$$\phi_s = -2\mathrm{Re}(F)\cos\omega t - 2\pi\mathrm{Re}\left(\mathrm{e}^Z\right)\sin\omega t, \tag{20}$$

$$\phi_d = \left[-2\frac{z}{r^2} - 2K\mathrm{Re}(F')\right]\cos\omega t - 2\pi K\mathrm{Re}\left(\mathrm{e}^Z\right)\sin\omega t, \tag{21}$$

$$\phi_q = -2K^2\mathrm{Re}(F'')\cos\omega t - 2\pi K^2\mathrm{Re}\left(\mathrm{e}^Z\right)\sin\omega t. \tag{22}$$

Using [17], equation 5.1.27 to evaluate

$$F' = F - Z^{-1}$$

and

$$F'' = F' + Z^{-2} = F - Z^{-1} + Z^{-2},$$

it follows that

$$\phi_d = -2K\mathrm{Re}(F)\cos\omega t - 2\pi K\mathrm{Re}\left(\mathrm{e}^Z\right)\sin\omega t = K\phi_s \tag{23}$$

and

$$\begin{aligned}\phi_q &= -2K^2\mathrm{Re}(F - Z^{-1} + Z^{-2})\cos\omega t - 2\pi K^2\mathrm{Re}\left(\mathrm{e}^Z\right)\sin\omega t \\ &= K^2\phi_s + 2K^2\mathrm{Re}(Z^{-1} - Z^{-2})\cos\omega t,\end{aligned} \tag{24}$$

or, equivalently,

$$\phi_q = K^2\phi_s - 2\left[K\frac{\cos\theta}{r} + \frac{\cos 2\theta}{r^2}\right]\cos\omega t, \tag{25}$$

where θ is the polar angle measured from the vertical line below the singularity.

The potential in square brackets in (25) is a wave-free singularity, with a dipole moment which cancels the corresponding moment from the first term. Thus the quadrupole is equivalent to the combination of the source and wave-free singularity with zero dipole moment, as stated in the Introduction.

Equation (23) can be derived more directly from the free-surface boundary condition, using reciprocity of the source potential; it follows that

$$K\phi_s - \frac{\partial \phi_s}{\partial \zeta} = 0 \quad \text{on} \quad \zeta = 0. \tag{26}$$

Thus the source and vertical dipole are duplicative when constructing a potential from singularities in the free surface, and the quadrupole is the next significant component of a multipole expansion.

Appendix B – Three-dimensional singularities in the free surface

Extending the notation from Appendix A, the source is situated at the point $x = \xi, y = \eta, z = \zeta$. Using results from [23], the Green function or source potential can be expressed in the form

$$G = [1/R + KF(X,Y)] \cos \omega t + 2\pi \mathrm{i} K \mathrm{e}^{-Y} J_0(X) \sin \omega t, \tag{27}$$

where

$$R = \sqrt{(x-\xi)^2 + (y-\eta)^2 + (z-\zeta)^2},$$
$$X = K\sqrt{(x-\xi)^2 + (y-\eta)^2},$$
$$Y = K|z+\zeta|,$$

and

$$F = \left(X^2 + Y^2\right)^{-1/2} - \pi \mathrm{e}^{-Y} \left[\mathbf{H}_0(X) + Y_0(X)\right] - 2\int_0^Y \mathrm{e}^{t-Y} \left(X^2 + t^2\right)^{-1/2} dt. \tag{28}$$

J_0, Y_0 and $\mathbf{H}_0$ are the Bessel and Struve functions of order zero [17].

The partial derivatives of F and G with respect to the vertical coordinate can be evaluated recursively. In particular, for the case $\zeta = 0$,

$$G_z = 2\frac{\partial}{\partial z} R^{-1} + KG \tag{29}$$

$$G_{zz} = 2\frac{\partial^2}{\partial Z^2} R^{-1} + KG_z = 2\left[\frac{\partial^2}{\partial z^2} R^{-1} + K\frac{\partial}{\partial z} R^{-1}\right] + K^2 G, \tag{30}$$

and so forth.

For $KR >> 1$ the integral in (28) can be expanded asymptotically in spherical harmonics, with the leading terms

$$\int_0^Y \mathrm{e}^{t-Y} \left(X^2 + t^2\right)^{-1/2} dt \simeq \sum_{n=0} n! P_n(\cos\theta)(KR)^{-(n+1)}. \tag{31}$$

Here θ is the angle measured to the field point from the negative z-axis. Thus, except for the radiated waves on the free surface, the Green function is dipole-like for $KR >> 1$,

$$G \simeq -\frac{2\cos\theta}{KR^2} \cos \omega t, \tag{32}$$

and the quadrupole G_{zz} is of order R^{-4}. The potential in square brackets in (30) is a wave-free singularity, with a dipole moment which cancels the corresponding moment from the last term. Thus the quadrupole is equivalent to this combination of the source and wave-free singularity, as noted above for the two-dimensional case.

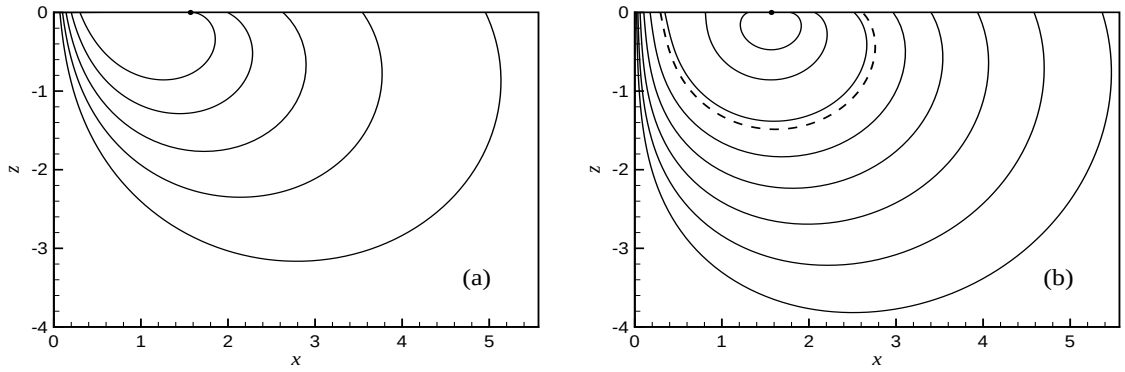

Figure 1: Streamlines generated by sources of strength $S = 1$ with $Q = V = 0$ (a) and quadrupoles of strength Q with $S = 0$ (b). The profiles in (a) are generated with starting values on the left waterline between $x = 0.07$ and $x = 0.30$. The dashed curve in (b) is for $Q/V = 1$ and the solid curves range from $Q/V = 0.04$ to 32, corresponding to the family of profiles in [13]. The singular point $(\pi/2, 0)$ is marked by a filled circle. Reflected streamlines for $x < 0$ are not shown.

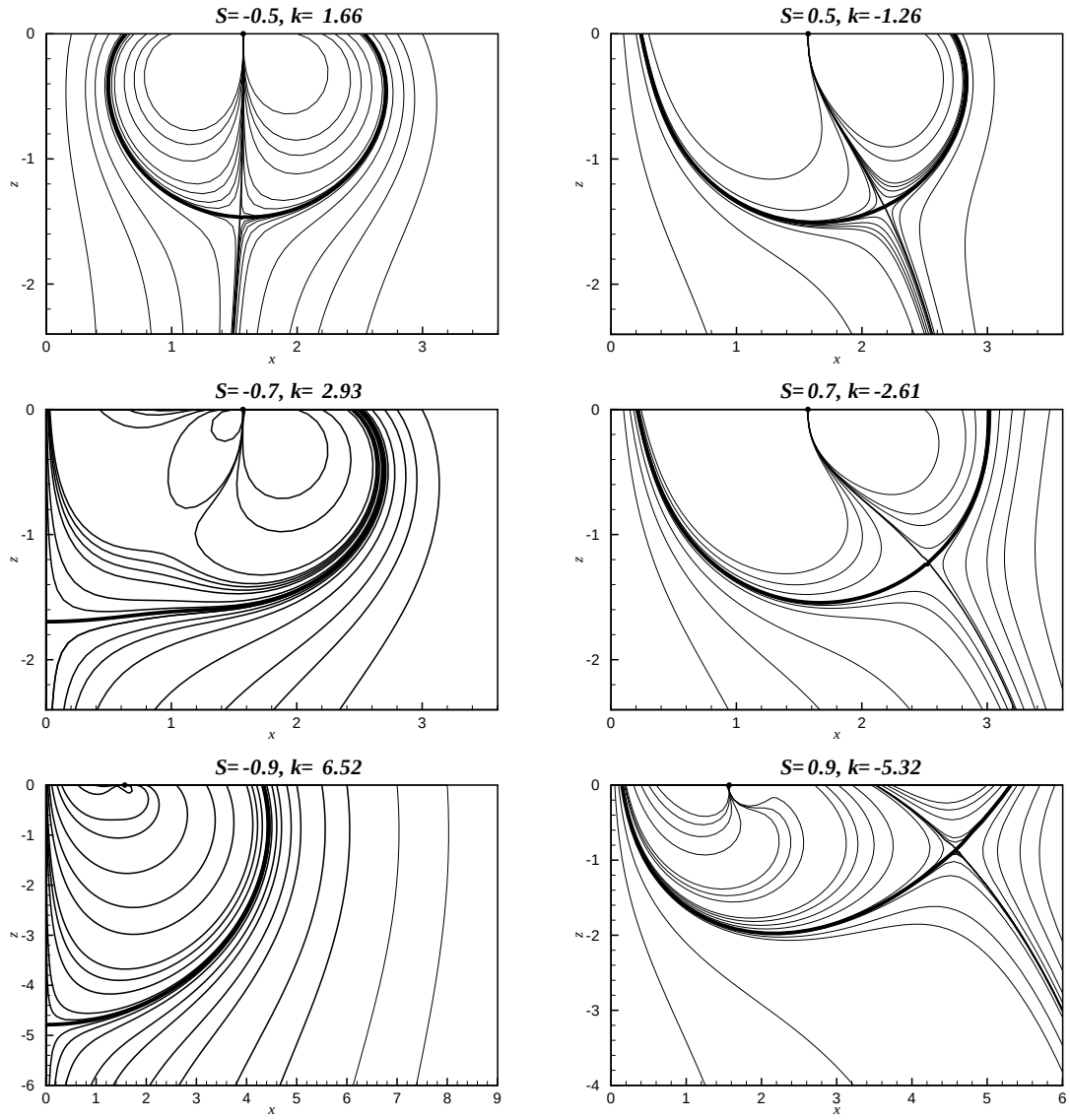

Figure 2: Streamlines generated by the complex potential (7) with $Q = V = 1 - |S|$. The body profile, shown by the heavy line, corresponds to the streamline which surrounds the singular point at $x = \pi/2$. The dividing streamline intersects this streamline normally at the stagnation point, and terminates at the singular point. The singular point $(\pi/2, 0)$ is marked by a filled circle. Reflected streamlines for $x < 0$ are not shown.

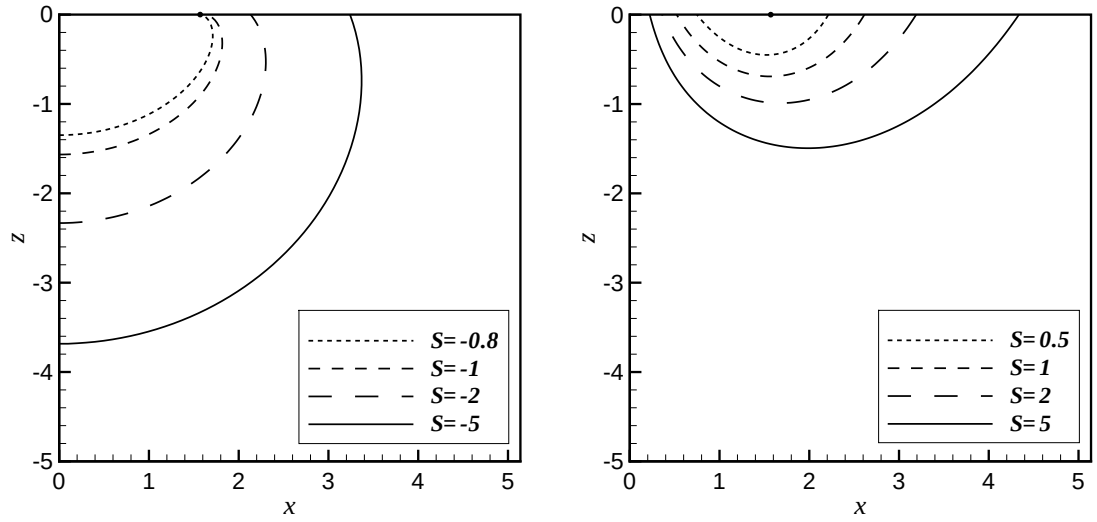

Figure 3: Streamlines generated by sources of strength S interacting with the vertical streaming flow $V = 1$. The quadrupole strength $Q = 0$. The profiles on the left are for $S < 0$ (sources with positive flux). The profiles on the right are for $S > 0$ (sinks). The singular point $(\pi/2, 0)$ is marked by a filled circle. Reflected streamlines for $x < 0$ are not shown.

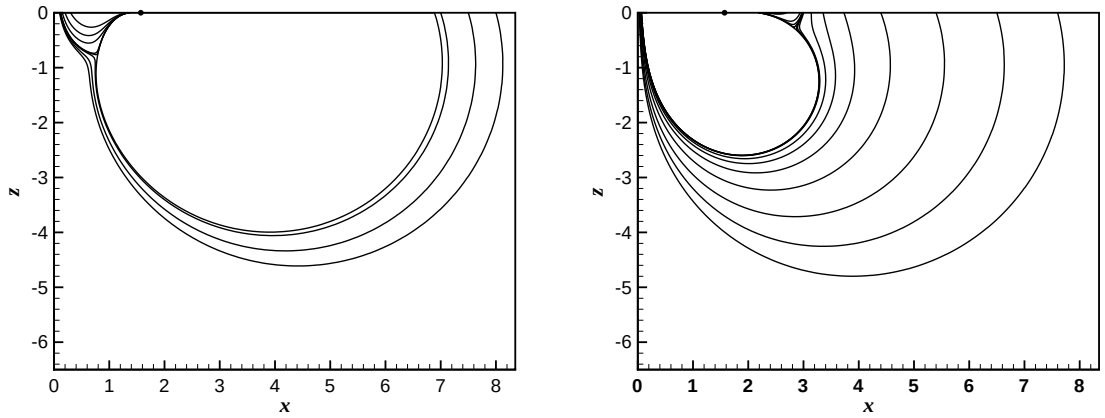

Figure 4: Streamlines generated by sources of strength S and quadrupoles of strength Q, with $V = 0$. The profiles on the left are for $Q/S = -0.5$, and on the right for $Q/S = +0.5$. Note the stagnation points on the innermost body profile. The singular point $(\pi/2, 0)$ is marked by a filled circle. Reflected streamlines for $x < 0$ are not shown.

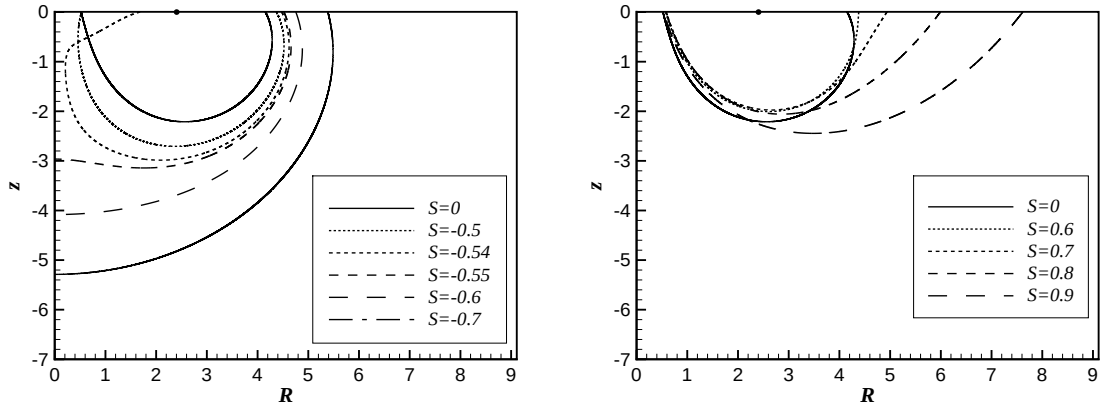

Figure 5: Profiles of axisymmetric structures with $Q = V = 1 - |S|$. The singular point at the radius $j_{0,1} = 2.4048..$ is marked by a filled circle.

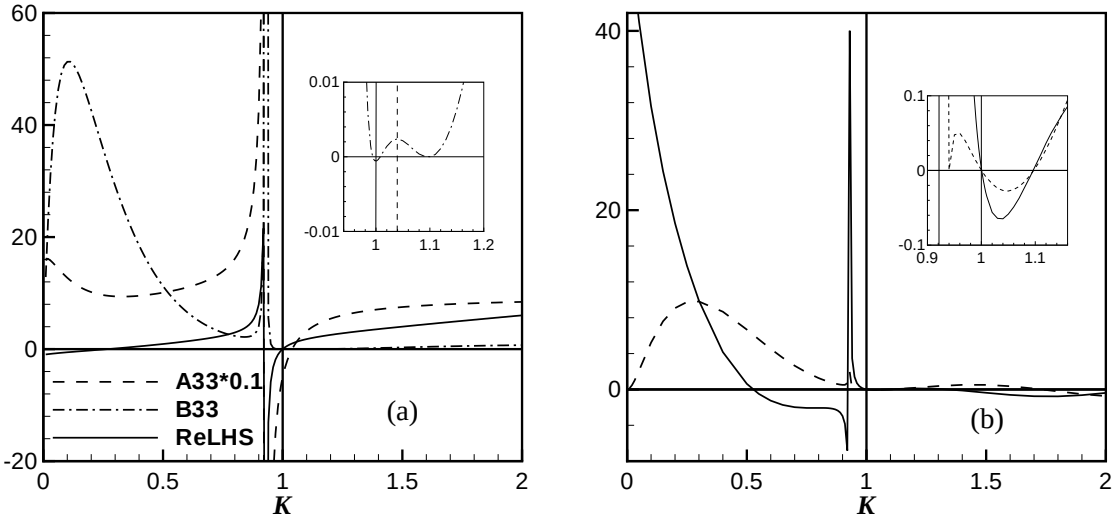

Figure 6: Hydrodynamic force coefficients for the axisymmetric profile $S = 0$. The coefficients in (a) are the added mass (A33), damping (B33), and real part of the equation of motion left-hand side (ReLHS). The coefficients in (b) are the real (solid) and imaginary (dashed line) parts of the exciting force. The insets show zoom plots of the coefficients near the trapping wavenumber $K = 1$.

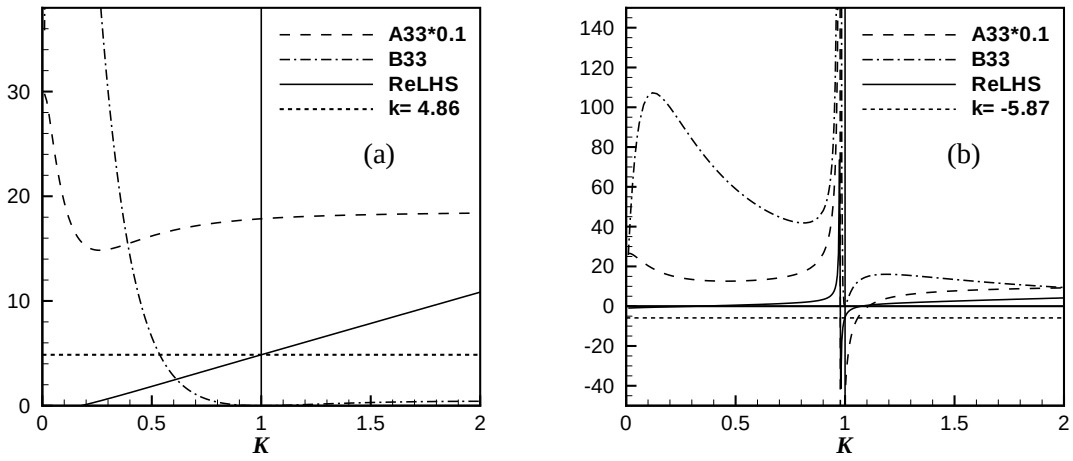

Figure 7: Added mass and damping coefficients, and real part of the equation of motion left-hand side for the axisymmetric profiles $S = -0.7$ (a) and $S = +0.7$ (b), with $Q = V = 0.3$. The damping coefficient in (a) has a peak value equal to 104, near $K = 0.1$. The horizontal dashed line is the value of the restoring coefficient k derived from equation 15.